# First steps with HLLMHD and PP reconstruction: Part II

by *O. Steiner, P. Rajaguru,* and *G. Vigeesh*

This is a continuation of part I of this report. In this second part we concentrate on the total radiative output at the top boundary as a function of time and on some horizontally averaged quantities as a function of height and of time. We also ran a model from Matthais Steffen (`d3t50g45mm00n04`) with $T_{\rm eff} = 5000$ K and $\log g = 4.5$ (compared to 5770 and 4.44 for the Sun). This cooler model has $n1 \times n2 \times n3 = 140 \times 140 \times 141$ grid cells. The size of the box is 4.942 Mm $\times$ 4.942 Mm $\times$ 2.4544 Mm. The $\tau = 1$ level is at a height of about 1.76 Mm from the bottom. The grid cells have a horizontal width of 35.3 km and a vertical extent varying from 64.3 km in the bottom part of the convection zone to $\approx 10$ km in the top part of the convection zone and down to 7.38 km in the top part of the box. The initial model consists of relaxed convection as computed with Roe and Van Leer reconstruction. The initial magnetic field (if not set zero) is homogeneous and vertical with a strength of 50 G.

Table 1 gives a compilation of all the models discussed in part I of this report and the new models with $T_{\rm eff} = 5000$ K. We also add at the top of the table some models from previous runs, which are used in the following analysis.

| job | solver | reconstr. | N_ordCT | $\nu_{\rm art.}$ | $B_{\rm init}$ [G] | initial model | $t_{\rm end}$ [s] |
|---|---|---|---|---|---|---|---|
| job3DB0 | HLLMHD | VanLeer | 1 | 0.0 | $B_z = 0$ | rmhd240x240x120 | 6011 |
| job3Dv50 | HLLMHD | VanLeer | 1 | 0.0 | $B_z = 50$ | rmhd240x240x120 | 6069 |
| job3Dh50 | HLLMHD | VanLeer | 1 | 0.0 | $B_h = 50$ | rmhd240x240x120 | 12023 |
| job_pp_hancock | HLLMHD | PP | 1 | 0.0 | $B_z = 50$ | rmhd120x120x120_v50 | 540 |
| Nord_ConsTrans | HLLMHD | PP | 2 | 0.0 | $B_z = 50$ | rmhd120x120x120_v50 | 540 |
| job_ifort | HLLMHD | PP | 1 | 0.0 | $B_z = 50$ | rmhd120x120x120_v50 | 540 |
| job_pp_hancock_nu0p5 | HLLMHD | PP | 1 | 0.5 | $B_z = 50$ | rmhd120x120x120_v50 | 540 |
| job_vanleer_hancock | HLLMHD | VanLeer | 1 | 0.0 | $B_z = 50$ | rmhd120x120x120_v50 | 540 |
| job_pp_eint | HLLMHD | PP | 2 | 0.0 | $B_z = 50$ | rmhd120x120x120_v50 | 540 |
| job3dB0 | HLLMHD | PP | 2 | 0.0 | $B_z = 0$ | rmhd240x240x120 | 2405 |
| job3dRoe | Roe | VanLeer | — | 0.0 | — | rhd240x240x120 | 3606 |
| job_d3t50g45mm00n04 | HLLMHD | PP | 2 | 0.0 | $B_z = 0$ | d3t50g45mm00n04_B0 | 7446 |
| job_d3t50g45mm00n04_v50 | HLLMHD | PP | 2 | 0.0 | $B_z = 50$ | d3t50g45mm00n04_v50 | 10163 |
| job_d3t50g45mm00n04_Roe | Roe | VanLeer | — | 0.0 | — | d3t50g45mm00n04.1079820 | 6163 |

Table 1: Model simulations. For job_pp_eint, beta_inv was set 0.0. In all other cases beta_inv=10.0

### Radiative flux at the top boundary

Figure 1 shows the total radiative output at the top in units of $\sigma T_{\rm eff}^4$. The green, black, and red curves refer to results from `job3DB0`, `job3dB0`, and `job3dRoe`, respectively. These are all solar models with a box of n1 $\times$ n2 $\times$ n3 $= 240 \times 240 \times 120$ grid cells and dimension 9.6 Mm $\times$ 9.6 Mm $\times$ 2.8 Mm. For `job3DB0`, $s_{\rm inflow} = 1.775 \times 10^9 =$ constant. This value was also used for `job3dB0` up to 1202 s but then it was switched to $s_{\rm inflow} = 1.773 \times 10^9$. Similarly, `job3dRoe` was run with $s_{\rm inflow} = 1.775 \times 10^9$ up to $t = 1201.7$ s and then, this value was switched to $s_{\rm inflow} = 1.773 \times 10^9$. The curves do not differ substantially from each other, which indicates that the radiative output does not strongly depend on whether we choose HLLMHD or the Roe solver, nor does it seem to depend on the reconstruction method VanLeer or PP. The plot also shows that 6000 s are still not a sufficiently long period for obtaining a reliable value for the effective temperature of the model.

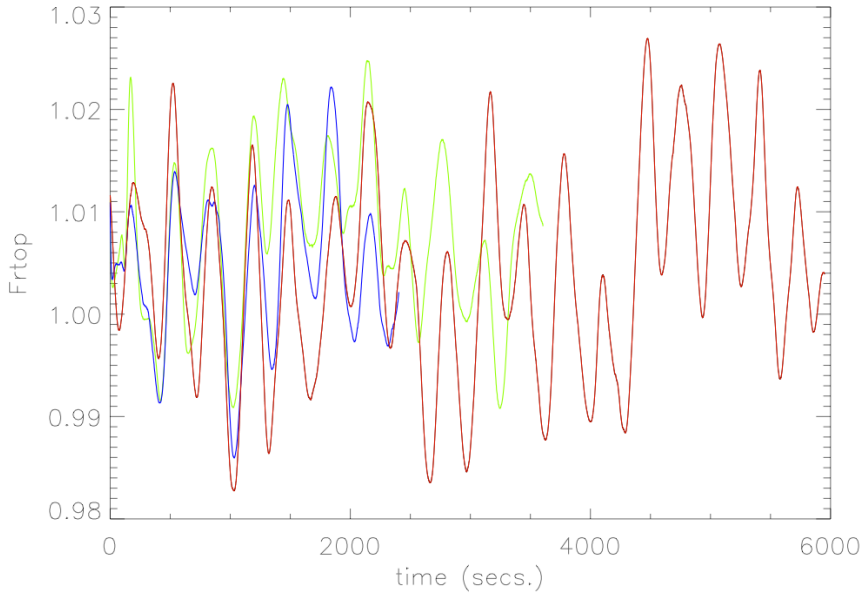


Figure 1: Bolometric radiative flux through the top boundary, Frtop, in units of $\sigma T_{\rm eff}^4$ as a function of time. Blue: HLLMHD+PP, green: Roe+VanLeer, Red: HLLMHD+VanLeer. Solar model with a box of n1 $\times$ n2 $\times$ n3 $= 240 \times 240 \times 120$ grid cells and dimensions 9.6 Mm $\times$ 9.6 Mm $\times$ 2.8 Mm. No magnetic field.

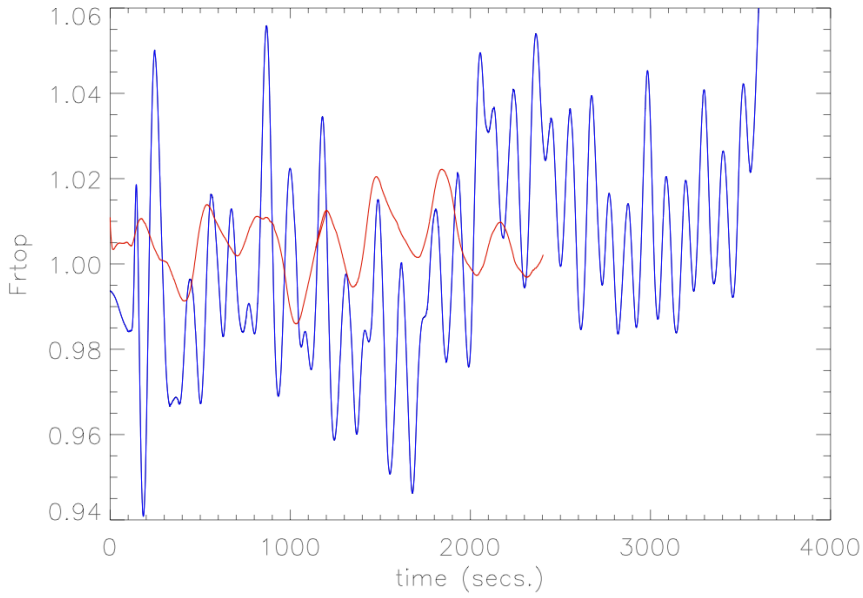


Figure 2: Bolometric radiative flux through the top boundary, Frtop, in units of $\sigma T_{\rm eff}^4$ as a function of time. Red: Sun, blue: model d3t50g45mm00n04. Both are computed with HLLMHD+PP with $\mathbf{B} = 0$.

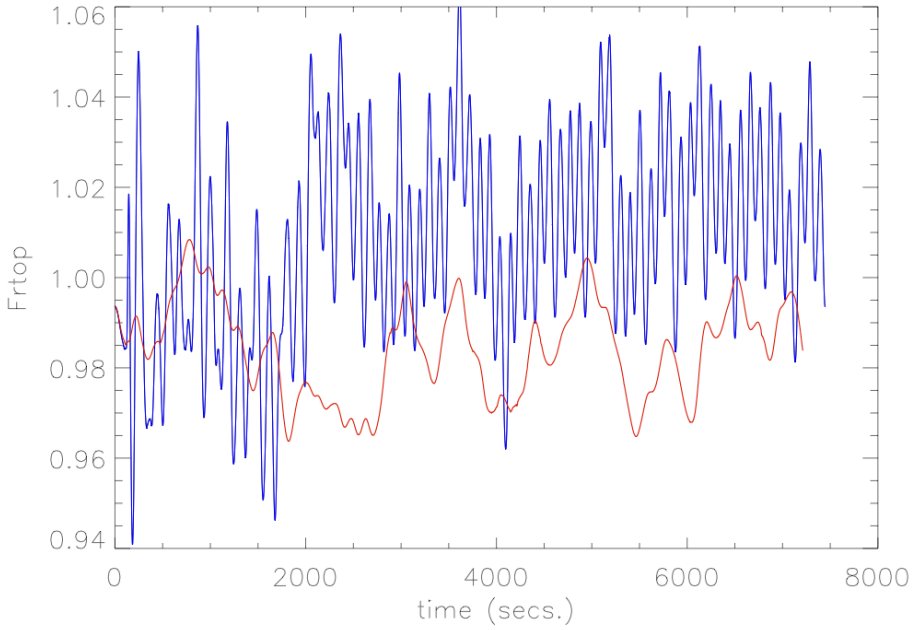


Figure 3: Bolometric radiative flux through the top boundary, Frtop, in units of $\sigma T_{\rm eff}^4$ as a function of time. Blue: HLLMHD+PP, red: Roe solver with VanLeer. For both runs with model d3t50g45mm00n04 with $\mathbf{B} = 0$ (for HLL) or no magnetic field at all (for Roe).

Figure 2 shows the total radiative output at the top in units of $\sigma T_{\rm eff}^4$ for the Sun (red) and for Model `d3t50g45mm00n04` (blue), both computed with HLLMHD+PP and $\mathbf{B} = 0$. The solar box (`job3dB0`) was approximately four times larger than the stellar box (`job_d3t50g45mm00n04`). The red curve in Fig. 2 is identical to the blue curve in Fig. 1. Two things are immediately apparent. The stellar model has larger amplitude ($\approx 6\%$ vs. $\approx 2\%$ for the Sun) and shorter period ($\approx 2\,\mathrm{min} = 8.3\,\mathrm{mHz}$ vs. $\approx 5.5\,\mathrm{min} = 3\,\mathrm{mHz}$ for the Sun). In order to find out if this large amplitude is an artifact of the HLL solver, we also ran the same stellar box with the Roe solver with VanLeer reconstruction.

Figure 3 shows the result. Clearly, the Roe solver does hardly show the p-mode oscillation—the fluctuation with an amplitude of about 2% is probably due to granular evolution. Thus, it seems that the strong oscillation in the simulation with HLLMHD is due to this solver. On the other hand, it seems like a paradox that the p-mode oscillations are clearly present for the solar model when computed with the Roe solver as can be seen from Fig. 1—in other words, we don't really know which of the two curves in Figure 3 is more faithful. Maybe some upper limit for this radiative fluctuation may come from observation?

### Mass fluxes

We also looked at oscillations in the mass flux. Fig. 4 shows the horizontally averaged, vertical mass flux at a level of $\langle\tau\rangle = 1$ as a function of time for the solar model `job3dB0` (red) and for the stellar model `job_d3t50g45mm00n04` (blue) both again with $\mathbf{B} = 0$ and computed with HLLMHD+PP. As in Fig. 2, the stellar model oscillates with a larger amplitude than the solar model does but not so drastically different as for Frtop, especially when considering that the density at $\langle\tau\rangle = 1$ is about $4.5 \times 10^{-7}$ g cm$^{-3}$ for the stellar model and $2.3 \times 10^{-7}$ g cm$^{-3}$ for the Sun: almost two times smaller. Also different from Fig. 2, the solar and the stellar model oscillate with similar frequencies: $\approx 5.34$ min $= 3.07$ mHz for the solar model and $\approx 5.14$ min $= 3.24$ mHz for the stellar model. The oscillation of the stellar model seems to consists of a superposition of two slightly different frequencies as two peaks gradually moves with respect to each other and, which seems to produce a beat frequency. It is possibly these two frequencies, which produce the short period oscillation seen in Frtop (Figs. 2 and 3).

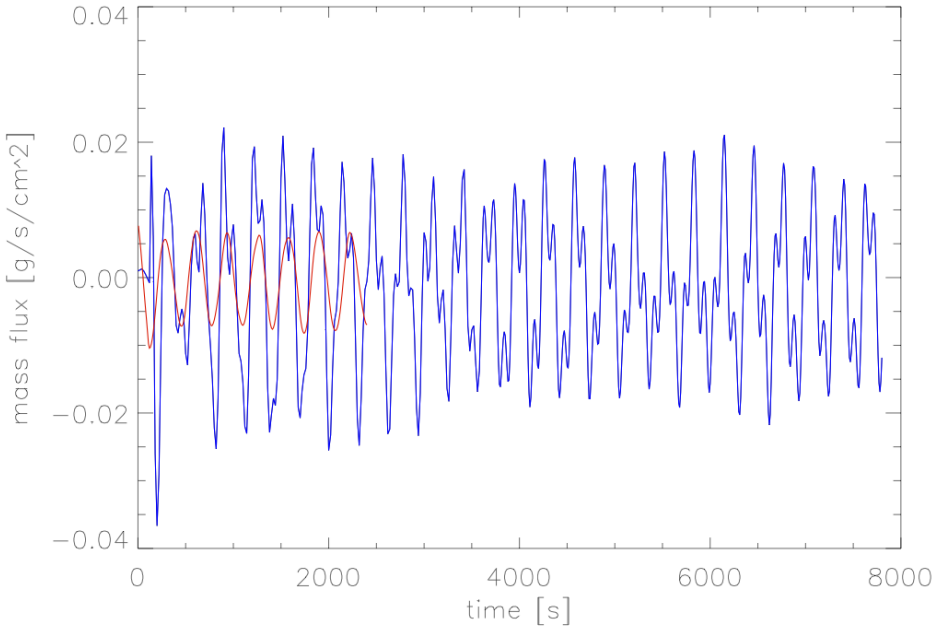


Figure 4: Horizontally averaged, vertical mass flux at a level of $\langle\tau\rangle = 1$ as a function of time. Red: Sun, blue: model d3t50g45mm00n04. Both are computed with HLLMHD+PP with $\mathbf{B} = 0$.

Fig. 5 shows the horizontally averaged, vertical mass flux at a level of $\langle\tau\rangle = 1$ as a function of time for the stellar model `job_d3t50g45mm00n04`, once computed with HLLMHD+PP (blue) with $\mathbf{B} = 0$ and once with the Roe solver (red) without magnetic field. This figure confirms the result from Fig. 3 in that the Roe solver produces much smaller oscillations than the HLL solver. Different from the oscillations

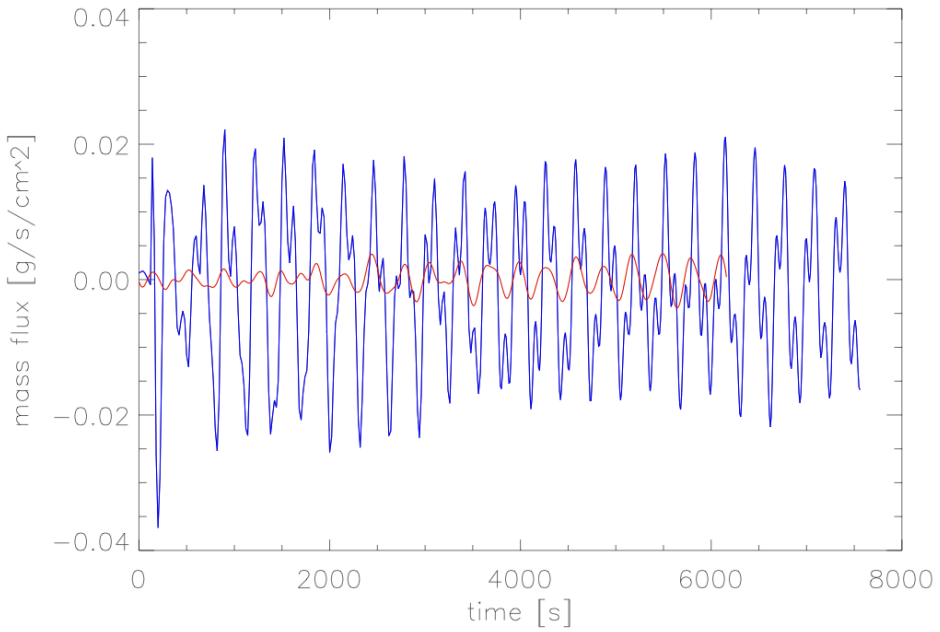


Figure 5: Horizontally averaged, verical mean mass flux at a level of $\langle\tau\rangle = 1$ as a function of time for model d3t50g45mm00n04. Blue: HLLMHD+PP and $\mathbf{B} = 0$, red: Roe solver with VanLeer and no magnetic field.

in Frtop (Fig. 3), the two models oscillate in phase after an initial transient phase of the simulation with the Roe solver.[1] Also note that the amplitude of the oscillations of the red curve seems to increase with time.

We can also do a similar comparison with two identical solar models, namely `job3dB0` for HLL+PP and `job3dRoe` for the Roe solver. This is shown in Fig. 6. Blue is with the Roe solver and VanLeer reconstruction and no magnetic field, red is with HLLMHD+PP and $\mathbf{B} = 0$. The two curves are very similar confirming the result of Fig. 1.

### Oscillations of the magnetic stellar model

We have also run the stellar model `d3t50g45mm00n04` comprising an initially homogeneous vertical magnetic field of a strength of 50 G. It seems that the magnetic field has a damping effect on the oscillations. This is apparent from Fig. 7, which shows the radiative flux through the top boundary in units of $\sigma T_{\rm eff}^4$ for the model with $T_{\rm eff} = 5000$ K. The green curve refers to the model without magnetic field computed with the Roe solver, the blue curve to the model with $\mathbf{B} = 0$ computed with HLLMHD+PP, and the red curve to the model with an initial homogeneous vertical magnetic field of 50 G computed with HLLMHD+PP. The amplitude of the fluc-

[1] This transient phase comes a bit as a surprise because the start model (job_d3t50g45mm00n04) is one that was previously computed with the Roe solver, however with an older version of the code but otherwise with the same parameter file.

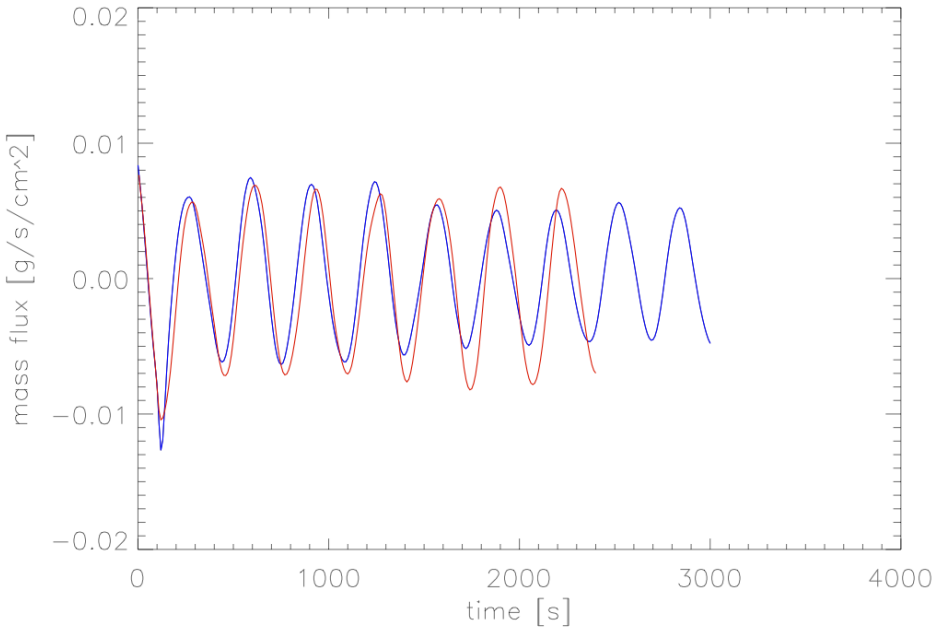


Figure 6: Horizontally averaged, vertical mass flux at a level of $\langle\tau\rangle = 1$ as a function of time for the solar model with n1 $\times$ n2 $\times$ n3 $= 240 \times 240 \times 120$. Red: HLLMHD+PP and $\mathbf{B} = 0$, blu: Roe solver with VanLeer and no magnetic field.

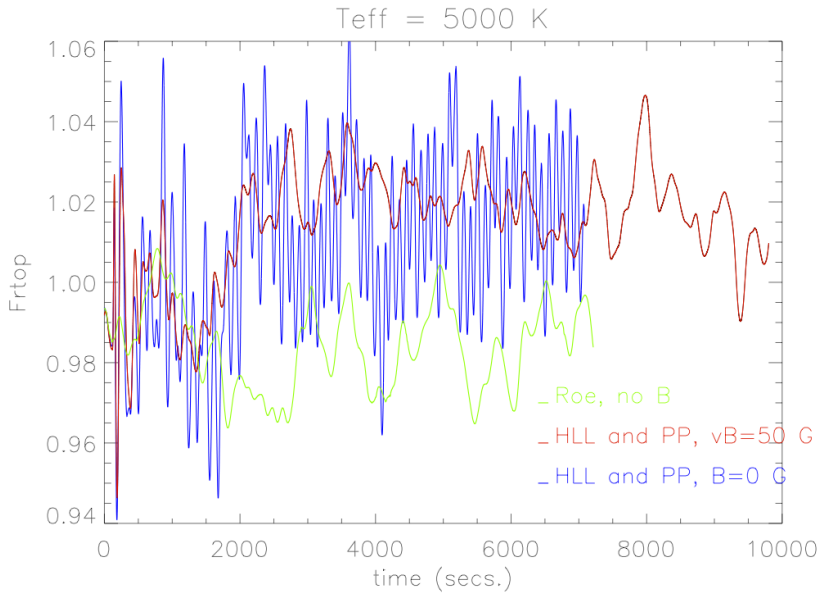


Figure 7: Radiative flux through the top boundary in units of $\sigma T_{\rm eff}^4$ as a function of time for the model with $T_{\rm eff} = 5000$ K. The green curve refers to the model without magnetic field computed with the Roe solver, the blue curve to the model with $\mathbf{B} = 0$ computed with HLLMHD+PP, and the red curve to the model with an initial homogeneous vertical magnetic field of 50 G computed with HLLMHD+PP.

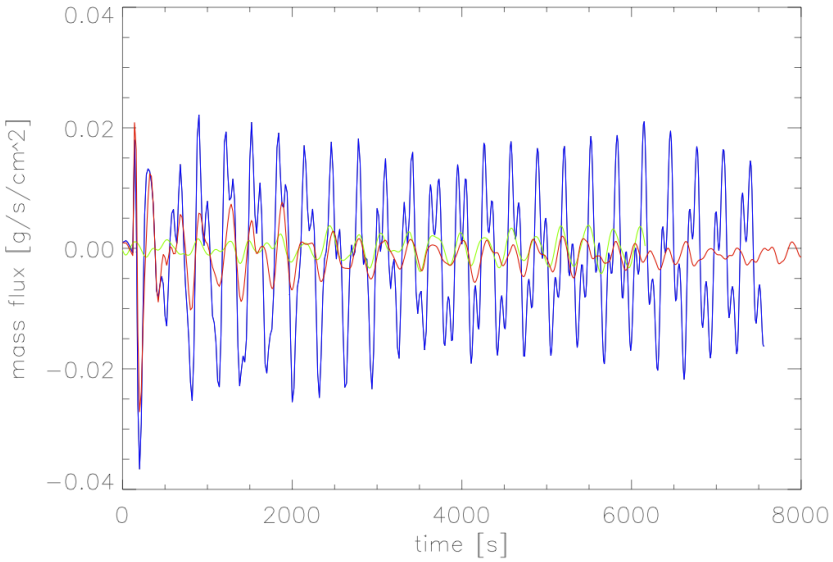


Figure 8: Horizontally averaged, vertical mass flux at a level of $\langle\tau\rangle = 1$ as a function of time for the model with $T_{\rm eff} = 5000$ K. The green curve refers to the model without magnetic field computed with the Roe solver, the blue curve to the model with $\mathbf{B} = 0$ computed with HLLMHD+PP, and the red curve to the model with an initial homogeneous vertical magnetic field of 50 G computed with HLLMHD+PP.

tuations of the red curve is initially similar to the blue curve but rapidly decreases showing a behavioure more like the green curve from the Roe solver. Initially, the amplitude is still large as long as the magnetic field is not yet concentrated in the intergranular lanes, which happens after $\approx 300$ sec. This damping effect of the magnetic field, however, takes longer when looking at the horizontally averaged mass flux as can be seen from Fig. 8. But after $\approx 6000$ s, the amplitude of the fluctuations stays very small. Regarding Fig. 7 it is noteworthy that HLLMHD seems to produce a higher effective temperature than the Roe solver, although we canot exclude that the green curve and the red curve may come closer together beyond 10000 s.

**Bolometric intensity maps**

Intensity maps from the solar models were discussed in part I of this report. Here we concentrate on the intensity maps from the stellar model with $T_{\rm eff} = 5000$ K. The oscillations of the model computed with HLLMHD+PP and $\mathbf{B} = 0$ have a particular side effect on the intensity maps. First of all, the overall intensity changes very quickly, which leads to a appreciable flickering in movies of the intensity. In particular, the brightness of the intergranular lanes changes drastically. This is shown in the time sequence of Fig. 9 (from top left to bottom right). First, the intergranular lanes show brighness almost like inverse granulation. 60 s later they are darker and look almost solar like to become bright again 60 s later and again back to normal. Instants of bright intergranular lanes correspond to peaks in Frtop in Fig. 7 and vice versa,

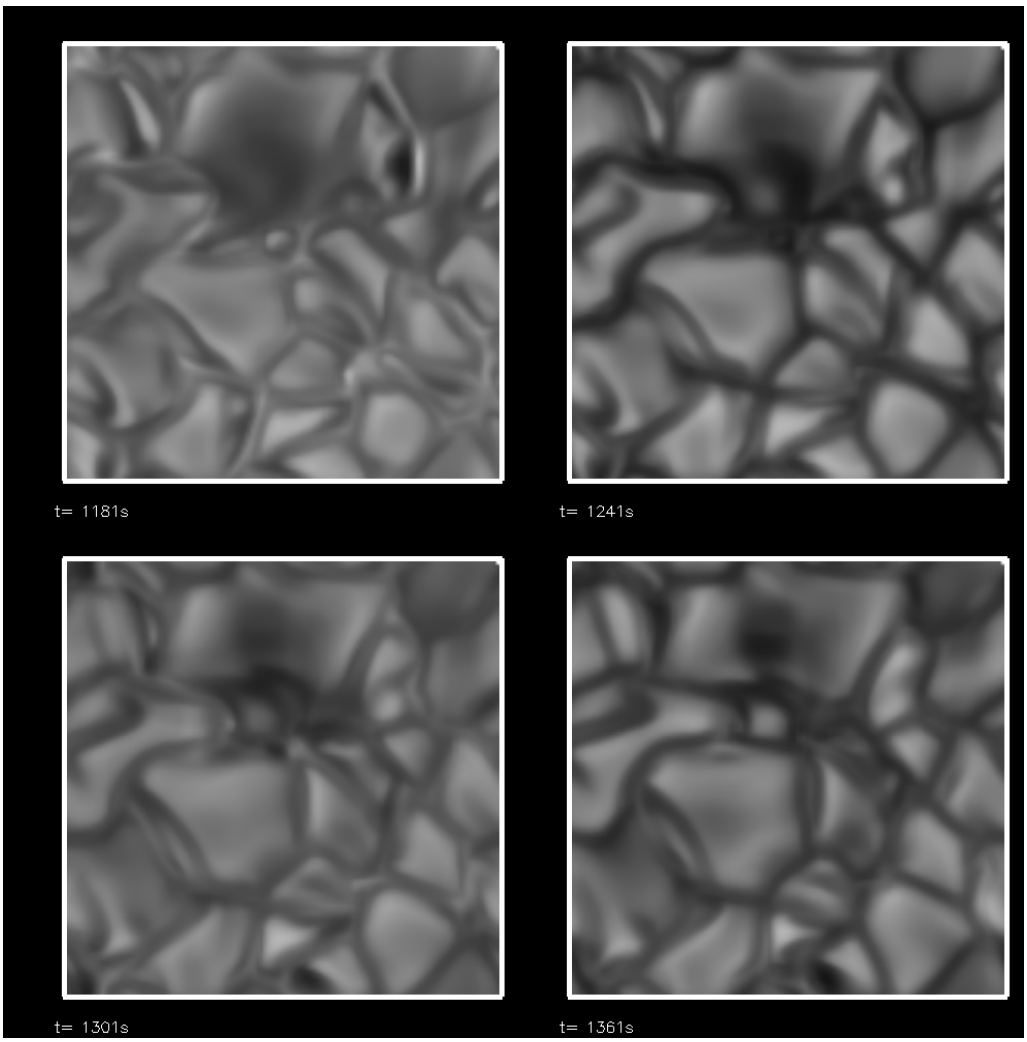


Figure 9: Time sequence (from top left to bottom right) of the bolometric intensity of the stellar model with $T_{\rm eff} = 5000$ K (d3t50g45mm00n04) with $\mathbf{B} = 0$ computed with HLLMHD+PP. The four snapshots are each 60 s apart. Black and white correspond to the same intensity level in each frame. Notice the change in intensity in the intergranular lanes.

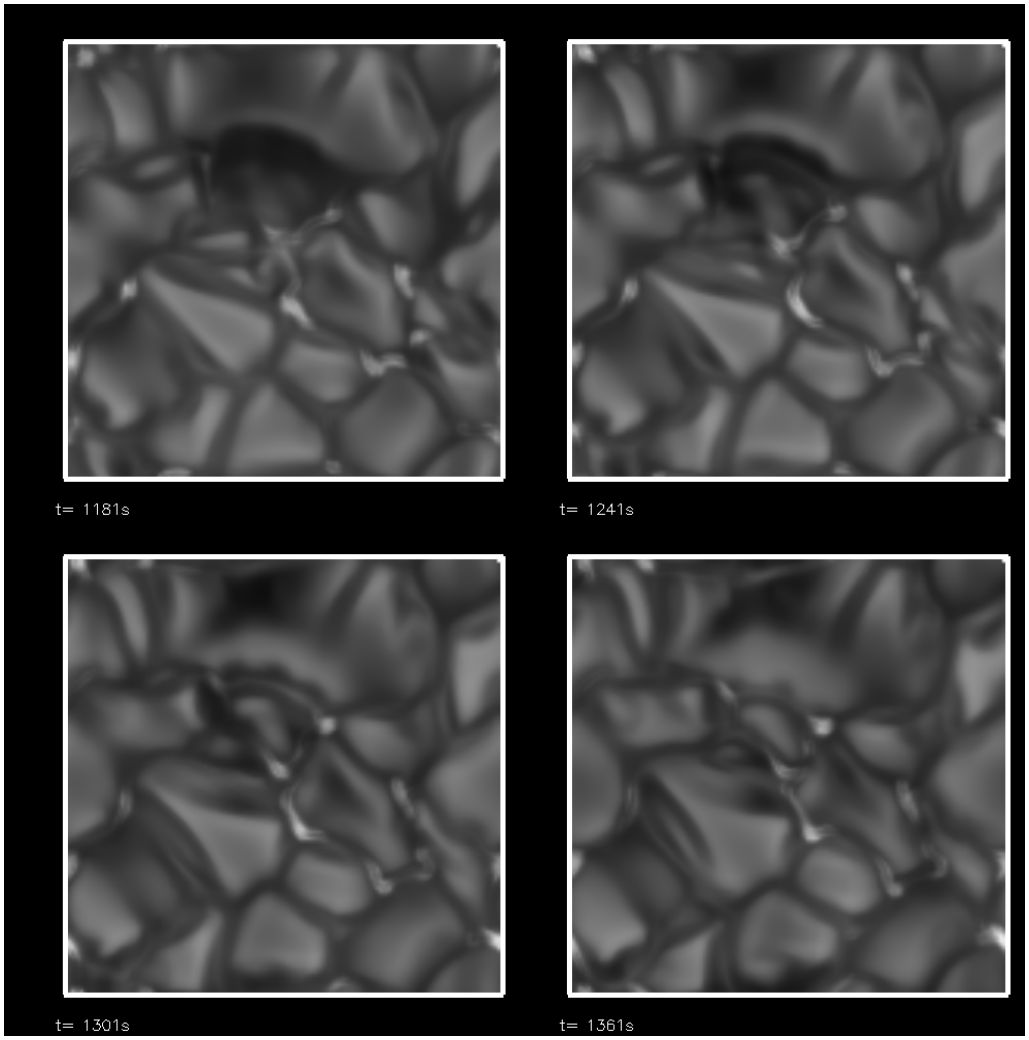


Figure 10: Time sequence (from top left to bottom right) of the bolometric intensity of the stellar model with $T_{\rm eff} = 5000$ K (d3t50g45mm00n04) with $\langle B_z \rangle = 50$ G computed with HLLMHD+PP. The four snapshots are each 60 s apart and at the same times as the snapshots of Fig. 9. Black and white correspond to the same intensity level in each frame. Notice the bright filigree, of magnetic field concentrations, which is due to the hot wall effect.

instants of dark intergranular lanes to minima in Frtop.

This is less a problem for the run with magnetic field as can be expected from Figs. 7 and 8. Fig. 10 shows the bolometric intensity maps for the same time instants as in Fig. 9. We see less overall intensity fluctuations and the intergranular lanes look less conspicuous. To some degree, the granular patter is still similar to the field-free run, even after 20 min real time simulation. However, the magnetic run clearly shows a bright filigree, of magnetic field concentrations, which is due to the hot wall effect. Single bright fibrils often consists of a double layer of bright filaments corresponding to the bright walls of a magnetic flux sheet. Presently, we do not know yet if a comparable solar model shows similar double layers and if they persists when increasing the number of ray directions in the radiative transfer (parameter `n_radtheta`). It is clear that they are barely resolved (they show the grid structure) so that higher spatial resolution is needed to render these structures more trustful.

**Mean vertical mass flux and velocity as a function of height**

Fig. 11 shows the mean vertical mass flux as a function of height $z$, $\langle \rho v_z \rangle(z)$ at three different time instances for the stellar simulation (`job_d3t50g45mm00n04`) as computed with HLLMHD+PP. The top panel corresponds to $t = 2100$ s, when the mean mass flow near $\langle \tau \rangle = 1$ is approximately zero (as can be seen see from Fig. 8). $\langle \tau \rangle = 1$ corresponds to $z = 0$. The bottom left panel corresponds to $t = 1860$ s, when $\langle \rho v_z \rangle(\langle \tau \rangle = 1)$ is strongly positive, and the bottom right panel corresponds to $t = 2000$ s, when $\langle \rho v_z \rangle(\langle \tau \rangle = 1)$ is strongly negative as can be seen from Fig. 8 as well. The red curve is the mass flux from the cell interfaces (`rhovb_xmean`), while the black curve is the cell centred mass flux (`rhov3_xmean`). We see strong wiggles in the latter mass flux. They seem to keep the same phase independent of wether the bulk of mass is flowing up or down and their wavelength is given by the cell width, $\Delta z$. It may be tempting to blame these wiggles for the strong oscillations in time of mass flux and radiative output of this simulation (Figs. 8 and Fig. 7). If so, the simulation with the Roe solver should not or less show these wiggles because it doesn't strongly oscillate. However, the absence of wiggles would not proof the above made conjecture.

Fig. 12 shows the mean vertical mass flux as a function of height $z$, $\langle \rho v_z \rangle(z)$, for the simulation with the Roe solver and time $t = 2100$s (corresponding to the top panel of Fig. 11). The corresponding curves for $t = 2000$ s and $t = 1860$ s look both very similar. The wiggles are, except for the lower most grid layer, absent, hence, Roe+VanLeer seems not to suffer from this problem. This speaks in favour of the conjecture that the wiggles are at the origin of the oscillations in Frtop and $\langle \rho v_z \rangle(t)$. In this case, Fig. 2 and Fig. 4 would suggest that the wiggles are a specific problem of the model `d3t50g45mm00n04` and should not occur for the solar models since these do not show strong oscillations. In order to check this, Fig. 13 shows $\langle \rho v_z \rangle(z)$ for a snapshot of the solar model `job3dB0`. The wiggles are also present but with a much lower amplitude than in the case of the stellar model. Again, this speaks in favour of the conjecture that the wiggles are at the origin of the oscillations.

If this is true, then Fig. 7 and Fig. 8 suggest that the stellar model with magnetic

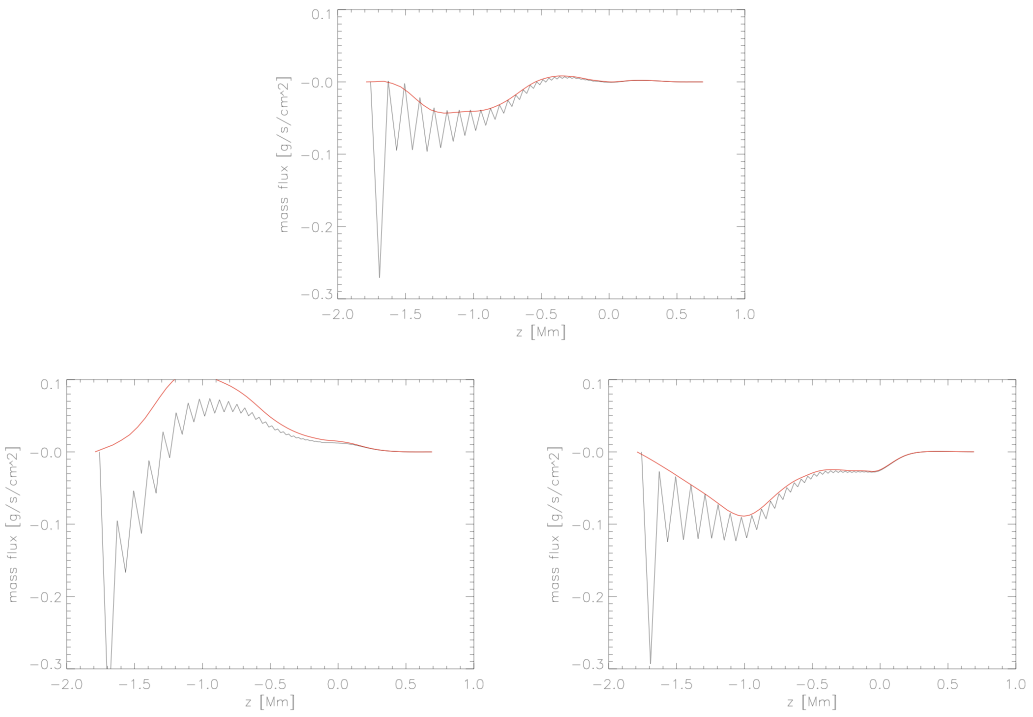


Figure 11: Horizontally averaged, vertical mass flux as a function of height $z$ at three different time instances for the stellar simulation ($T_{\rm eff} = 5000$ K) with HLLMHD+PP. *Top:* $t = 2100$ s, corresponding to an instant where the mean mass flow near $\langle\tau\rangle = 1$ is approximately zero (see Fig. 8). $\langle\tau\rangle = 1$ corresponds to $z = 0$. *Bottom left:* $t = 1860$ s, where $\langle\rho v_z\rangle(\langle\tau\rangle = 1)$ is strong positive. *Bottom right:* $t = 2000$ s, where $\langle\rho v_z\rangle(\langle\tau\rangle = 1)$ is strong negative. The black curve is the cell centred mass flux (rhov3_xmean), while the red curve is the mass flux from the cell interfaces (rhovb_xmean).

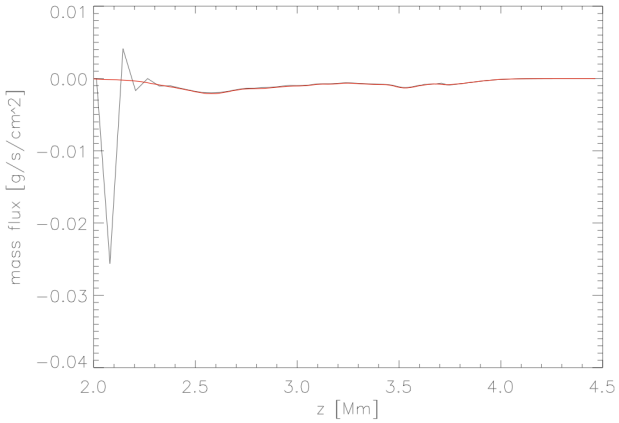


Figure 12: Horizontally averaged, vertical mass flux as a function of height $z$ at $t = 2100$ s for the stellar simulation ($T_{\rm eff} = 5000$ K) as computed with Roe+VanLeer. The black curve is the cell centred mass flux (rhov3_xmean), while the red curve is the mass flux from the cell interfaces (rhovb_xmean).

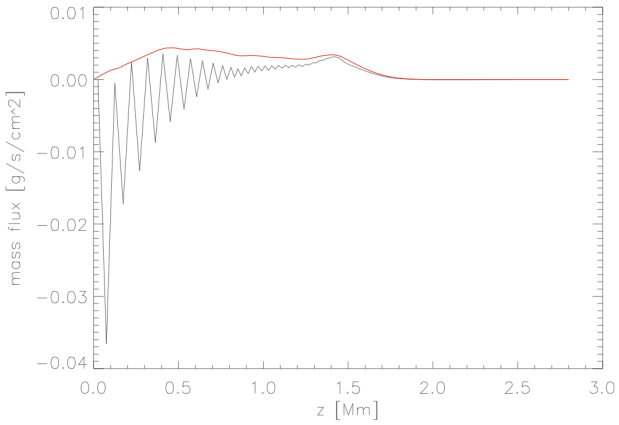


Figure 13: Horizontally averaged, vertical mass flux as a function of height $z$ at $t = 550$ s for the solar run job3dB0 as computed with HLLMHD+PP and $\mathbf{B} = 0$. Note that the scale of the mass flux is an order of magnitude smaller than in Fig. 11. The black curve is the cell centred mass flux (rhov3_xmean), while the red curve is the mass flux from the cell interfaces (rhovb_xmean).

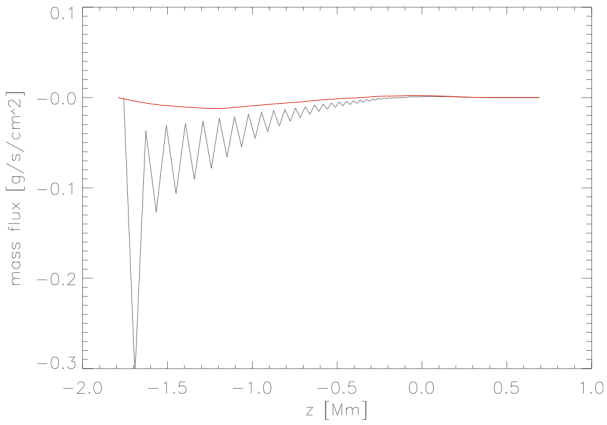


Figure 14: Horizontally averaged, vertical mass flux as a function of height $z$ at $t = 2100$ s for the stellar simulation ($T_{\rm eff} = 5000$ K) with a magnetic field, $\langle B_z \rangle = 50$ G computed with HLLMHD+PP. The black curve is the cell centred mass flux (rhov3_xmean), while the red curve is the mass flux from the cell interfaces (rhovb_xmean).

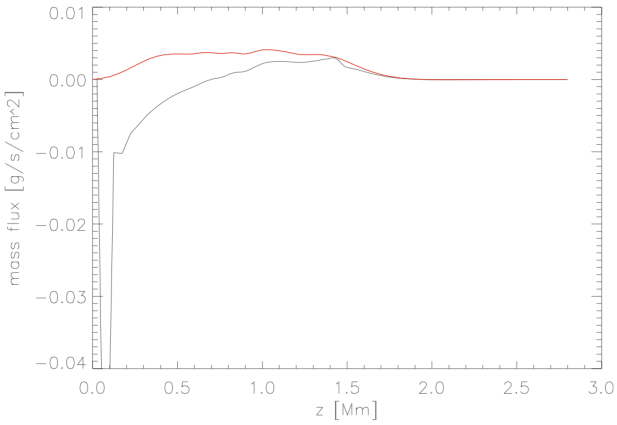


Figure 15: Horizontally averaged, vertical mass flux as a function of height $z$ at $t = 550$ s for the solar run job3DB0 as computed with HLLMHD+VanLeer and $\mathbf{B} = 0$. This is to compare with Fig. 13. The black curve is the cell centred mass flux (rhov3_xmean), while the red curve is the mass flux from the cell interfaces (rhovb_xmean).

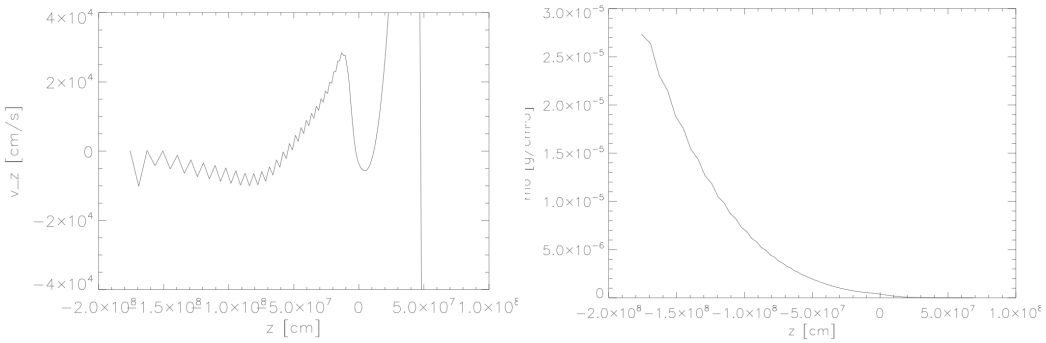


Figure 16: Horizontally averaged, vertical velocity (*left*) and density (*right*) as a function of height $z$ at $t = 2100$ s for the stellar simulation ($T_{\rm eff} = 5000$ K) with $\langle B_z \rangle = 0$ G computed with HLLMHD+PP.

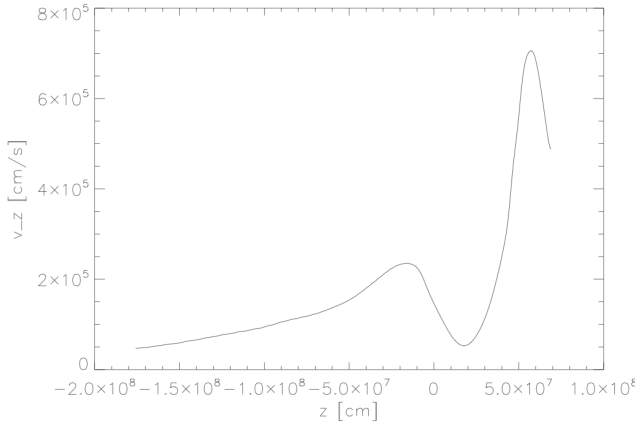


Figure 17: Horizontal rms of the vertical velocity (V3_XMEAN2) as a function of height $z$ at $t = 2100$ s for the stellar simulation ($T_{\rm eff} = 5000$ K) with $\langle B_z \rangle = 0$ G computed with HLLMHD+PP.

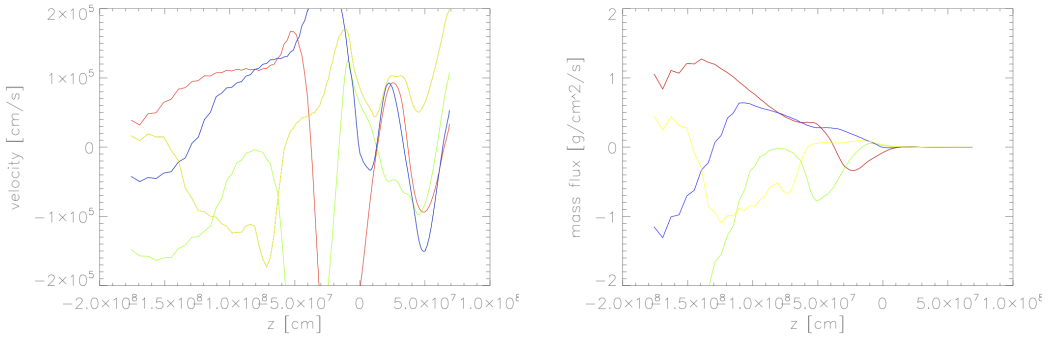


Figure 18: *Left:* Vertical velocity as a function of height $z$ at the four locations $(n_x, n_y) = (35, 35)$ (red), $(35, 105)$ (green), $(105, 35)$ (blue), and $(105, 105)$ (yellow). They refer to time $t = 2100$ s of the stellar simulation ($T_{\rm eff} = 5000$ K) with $\langle B_z \rangle = 0$ G computed with HLLMHD+PP. *Right:* Corresponding mass flux.

field does not (or less) suffer from the wiggles because the magnetic models show no strong oscillations. Fig. 14 shows that this is not the case. For the magnetic stellar atmosphere, the wiggles have as high an amplitude as for the model with $\mathbf{B} = 0$. But different from the model with $\mathbf{B} = 0$, the mass flux asymptotically approaches zero from negative values, while the non-magnetic model (see Fig. 11) overshoot and undershoot zero mass flux. The difference is even more striking when looking at the mass flux from the cell-interfaces (red curves): while the magnetic model shows this mass flux close to zero everywhere, the non-magnetic model shows stronger deviations from zero, which change as a function of time. Clearly, it is this overshooting and undershooting that causes the oszillation in Frtop and $\langle \rho v_z \rangle(t)$. For some reason, this oscillation is rapidly damped in the magnetic model and therefore, the oscillations in Frtop and $\langle \rho v_z \rangle(t)$ disappear, but the wiggles in $\langle \rho v_z \rangle(z)$ persist.

It would be interesting to know whether the wiggles persists when computing with HLLMHD+VanLeer. If yes, the wiggles must occur in connection with HLLMHD, if no, they occur in connection with PP. Unfortunately, we have no run of model `d3t50g45mm00n04` with HLLMHD+VanLeer but we have a solar model for comparison. The result for HLLMHD+PP was already shown in Fig. 13. Now, Fig. 15 shows the corresponding mean mass flux for the run with HLLMHD+VanLeer. It shows, that there are no wiggles, indicating that PP is the source of the problem. Fig. 15 shows a behaviour that is rather similar to the mean mass flux with the Roe solver (Fig. 12), except that the spike in the bottom layer is much larger, the mass flux does not stay as close to zero as in case of Fig. 12, and a difference between the black and the red curve persists throughout the convection zone.

There arises the question whether the wiggles in the mass flux come from the density (continuity equation) or from the velocity (momentum equation). Fig. 16 shows to the left the horizontal mean vertical velocity as a function of height for the model `d3t50g45mm00n04` computed with HLLMHD+PP for $t = 2100$ s. On the right, there is the corresponding density. The density shows also wiggles (they are not visible when plotting the logarithm of the density) but the velocity shows them

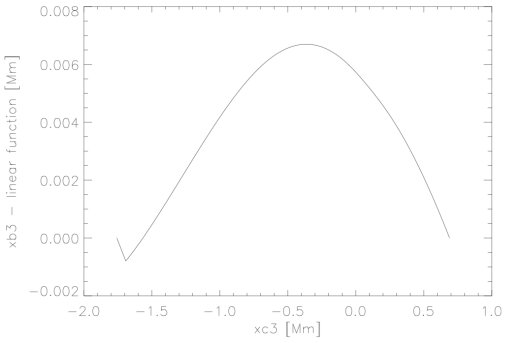


Figure 19: xb3 vs xc3 minus a linear function given by $\mathrm{xb3}(0)+\alpha\cdot(\mathrm{xc3}(i)-\mathrm{xc3}(0))$, where $\alpha=(\mathrm{xb3}(140)-\mathrm{xb3}(0))/(\mathrm{xc3}(140)-\mathrm{xc3}(0))$.

more clearly. Thus, it seems that the troubles come from the velocity not the density.

It should be mentioned that when plotting the rms of $v_z(z)$ (`V3_XMEAN2`), there are virtually no wiggles present. This is shown in Fig. 17.

Considering this, the question arises how the velocity or mass flux as a function of height looks like at a specific position in the horizontal plane. Fig. 18 (left) therefore shows the vertical velocity at four selected points in the box, i.e., at $(n_x,n_y)=(35,35)$, $(35,105)$, $(105,35)$, and $(105,105)$. We see that the wiggles are present, independently of whether there is a prevalent downnflow or prevalent upflow. We also see that they are more than an order of magnitude smaller than the actual velocities. Interestingly, they seem to be in phase with each other even though the four profiles were taken at largely different locations. The reason for the rms not showing the wiggles is probably due to the fact that there are approximately as much positive as negative velocities. Because the wiggles are in phase, wiggles in connection with negative velocities tend to cancel wiggles connected to positive velocities when computing the rms. Fig. 18 (right) shows the corresponding mass fluxes.

Since the wiggles occur in the cell centred mass fluxes only and not in the cell-interface mass fluxes, one might suspect that the wiggles arise merely because of the coordinates associated with cell centred quantities in relation to the coordinates associated with the cell boundaries. Fig. 19 shows this relationship for the model `d3t50g45mm00n04`. It is a smooth function and has no wiggles. Therefore, the wiggles cannot originate from this relationship.

In some sense, the mass fluxes at the cell boundaries can be considered more fundamental than the cell centred mass fluxes because it is the former that is used for updating the density when integrating the continuity equation. It should also be mentioned that the momentum flux, `frhov33b_xmean`, does not show any signs of wiggles. Therefore, it could well be that the wiggles seen in the cell centred mass flux and velocity is not a major problem after all.

**Strong difference in the flow and temperature structure of the upper atmosphere between magnetic and non-magnetic models.**

In part I of this report, we have shown horizontal sections of the temperature in the upper layers of the atmosphere, which strongly showed the grid structure, wiggles, and saw-teeths. Already in part I, we found that this problem only occurs in models with magnetic fields. Now we found (and it was previously noted by Shelyag et al. (2011, A&A 526, A5)) that models with magnetic fields show strong vorticity in the upper (chromospheric) layers. The velocity field in the top layers looks very different depending on whether there is a magnetic field present or not. Fig. 20 shows snapshot from the stellar model d3t50g45mm00n04 at an arbitrary time $t = 6500$ s. The left column shows the snapshot from the run with $\mathbf{B} = 0$ (job_d3t50g45mm00n04), the right column is from the model with $\langle B_z \rangle = 50$ G (job_d3t50g45mm00n04_v50) at the same time. Both simulations were computed with HLLMHD+PP. The top row shows the absolute magnetic field strength and the velocity field projected into the horizontal plane, which is located 615 km above $\langle \tau \rangle = 1$. The bottom row shows the temperature at the same level.

The difference between the field-free run and the run with magnetic field is conspicuous: not only in the velocity field but also in temperature. We see now that the problems with the temperature (grid structure, saw-teeth) occur in regions of strong vorticity. It seems they occur strongest where vertically oriented magnetic field is transported by horizontal vortical flows.

We mention here that we have carried out additional runs including magnetic diffusion with the hope to smooth the saw-teeth in temperature and internal energy. We experimented with parameters `c_resB`, `c_resepsilon`, and `c_resBconst`, however, without success.

**Conclusions**

We have carried out first 3-D stellar atmospheric simulations, which include magnetic fields, using the HLLMHD solver in conjunction with the piecewise parabolic (PP) reconstruction. Simulations were carried out for a stellar atmosphere with $T_{\rm eff} = 5000$ K and $\log g = 4.5$ (model `d3t50g45mm00n04` from Matthias Steffen). Looking first at the total radiative flux through the top boundary we find strong oscillations ($\approx 6\%$) of high frequency ($\approx 2$ min) when computing with HLLMHD+PP. The oscillations seem to be largely due to the intergranular lanes, which become bright and dark with this period. These oscillations are not present when doing the same simulation with the Roe solver and VanLeer reconstruction. We don't have similar problems with solar models for which oscillations in Frtop are similar for simulations with Roe or HLLMHD and VanLeer or PP. The problems are also absent when we add magnetic field to the stellar model. In this case, the high frequency oscillations disappear at once and the intergranular lanes don't flicker anymore.

Looking at the horizontally averaged mass fluxes at $\langle \tau \rangle = 1$, we recover a similar picture. Model `d3t50g45mm00n04` without magnetic field and computed with HLLMHD+PP shows strong oscillations, however with a more solar-like frequency

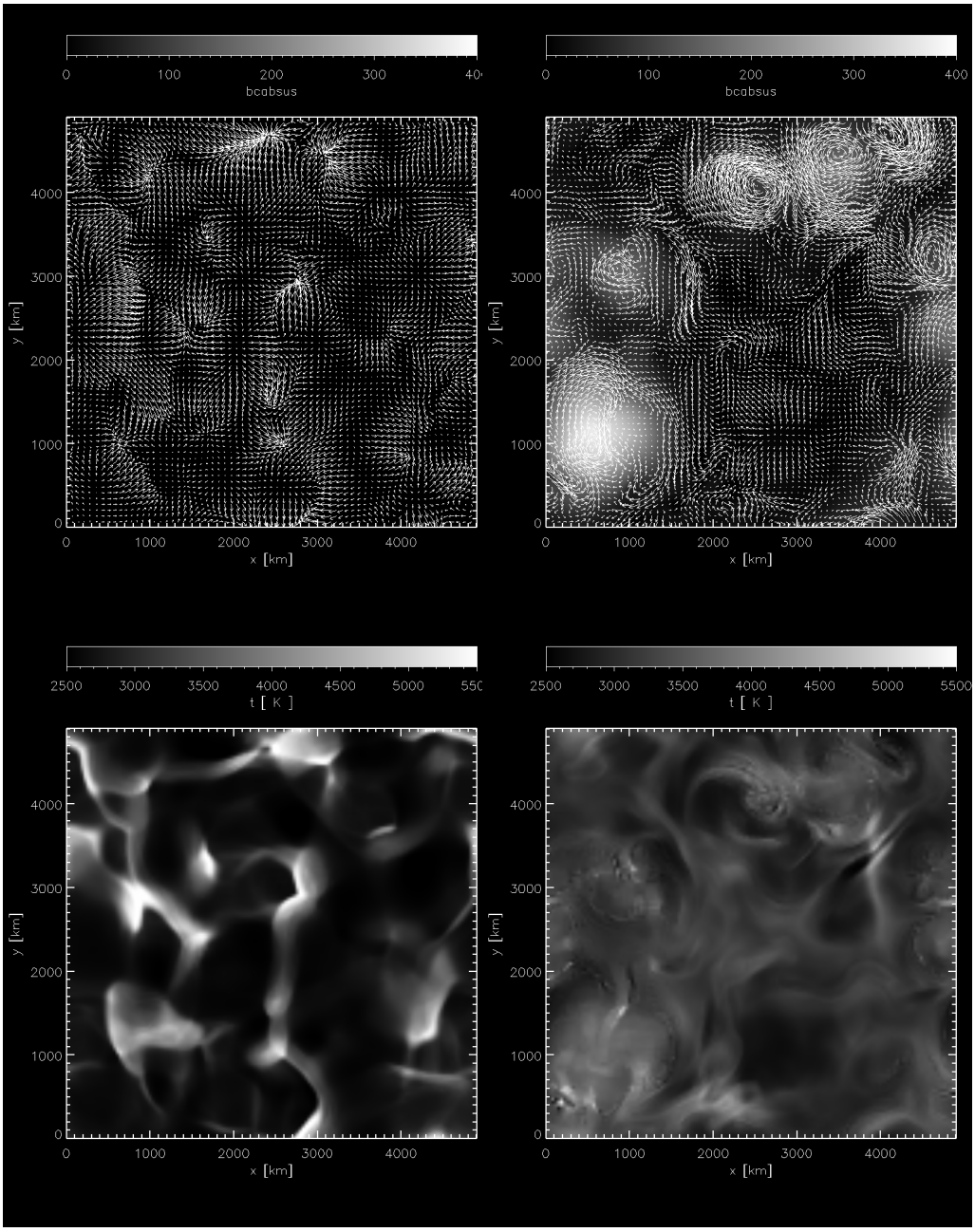


Figure 20: Snapshot from the stellar model d3t50g45mm00n04 at time $t = 6500$ s. The left column refers to the run with $\mathbf{B} = 0$ (job_d3t50g45mm00n04), the right column refers to the model with $\langle B_z \rangle = 50$ G (job_d3t50g45mm00n04_v50) both computed with HLLMHD+PP. The top row shows the absolute magnetic field strength and the velocity field projected into the horizontal plane, which is located 615 km above $\langle \tau \rangle = 1$. The bottom row shows the temperature at the same level. Note the drastic differences between the magnetic and non-magnetic model.

of 5.14 min. There seems to exist two modes of similar frequency, which might lead to a doubling in the oscillation frequency of Frtop. One mode might be associated with a global box p-mode the other with the intergranular down flows, which might less contribute to the mass flow at $\langle\tau\rangle = 1$ but still strongly influence Frtop. For the mass flux, the difference between the stellar model and the solar model is not as drastic as for the radiative flux but again, the solar models oscillate with a smaller amplitude. Again, for the solar model, there is no major difference when computing with Roe+VanLeer or HLLMHD+PP. And again, when introducing magnetic fields, the oscillations disappear at once and HLLMHD+PP and Roe+VanLeer produce a similar mass-flux oscillation at $\langle\tau\rangle = 1$.

The horizontally averaged vertical mass flux as a function of height in the atmosphere also shows striking differences between HLLMHD and Roe. The cell centred mass fluxes show wiggles with a wave length given by the cell size. These wiggles are absent for the mass fluxes at the cell boundaries. Only HLLMHD+PP show these wiggles, not the Roe solver. For the solar model the wiggles are also there but with an order of magnitude smaller amplitude. Also, HLLMHD+VanLeer does not show the wiggles (for a solar model), which brought us to the conclusion that they must be connected to the PP reconstruction. In contrast to what one might expect, these wiggles do not disappear with the introduction of a magnetic field. Since the magnetic field has led to the disappearance of the strong oscillations in the radiative flux at the top and in the mass flux at $\langle\tau\rangle = 1$, we conclude from this that the wiggles are probably not at the origin of these oscillations. Obviously, the wiggles that persists to be present in the magnetic model to not cause it to strongly oscillate. The wiggles in the mass flux seem to be due to wiggles in the velocity and they are in phase between different lines of sight through the box, meaning that they are a global phenomenon.

We found profound differences in flow and temperature structure in the upper layers of the atmosphere between the magnetic and the non-magnetic model. The magnetic model shows strong vortical flows in horizontal sections through the box. These flows are completely absent in the non-magnetic model. The non-magnetic model shows the usual network of shock fronts in horizontal sections of the temperature. These are less present in the model with magnetic field and the temperature field is more homogeneous. We find that these vortical flows are at the origin of problems concerning wiggles and saw-teeth in the temperature and internal energy of the model with magnetic field. It seems that the problem occurs because of the largely horizontal flow of the vortex carrying a vertically directed magnetic field.

**Appraisal and Outlook**

We have now gained some confidence in using HLLMHD with PP reconstruction for the model `d3t50g45mm00n04` with magnetic field. We consider the wiggles and saw-teeth in temperature and internal energy of the upper layers not to be a fundamental problem. It is certainly unaesthetic but not necessarily detrimental to the accuracy. The wiggles in mass flux and velocity as a function of height is really a problem only for the cell centred mass flux, not for the cell-boundary mass flux. Again, it may be not detrimental to the accuracy but it can be clearly seen as plane-parallel stairs in contour plots of the vertical mass flux or the vertical velocity in vertical

cross sections through the computational domain. More troublesome seem to us the big difference in oscillations of the radiative output and mass flux at $\langle\tau\rangle = 1$ between models computed with HLLMHD and models compudet with Roe. Fortunately, these oscillations disappear when introducing a magnetic field.

Recently, we have received more stellar models from Matthias Steffen complementing the model with $T_{\rm eff} = 5000$ K, viz., a model with $T_{\rm eff} = 4000$ K, one with $T_{\rm eff} = 6500$ K, and a solar model of similar size. We are planning to carry out further runs with these models. Ultimately, the plan is to investigate the structure and energetics of small-scale magnetic flux concentrations in these stellar atmospheres. In particular, we are interested in finding out about changes of the hot-wall effect as a function of stellar type. For this, however, we probably need to increase (double) the horizontal spatial resolution and we may want to increase the angular and possibly spatial resolution of the radiative transfer.

Freiburg. i. Br., 7. 8. 2011